

RSC Advances



This is an *Accepted Manuscript*, which has been through the Royal Society of Chemistry peer review process and has been accepted for publication.

Accepted Manuscripts are published online shortly after acceptance, before technical editing, formatting and proof reading. Using this free service, authors can make their results available to the community, in citable form, before we publish the edited article. This *Accepted Manuscript* will be replaced by the edited, formatted and paginated article as soon as this is available.

You can find more information about *Accepted Manuscripts* in the [Information for Authors](#).

Please note that technical editing may introduce minor changes to the text and/or graphics, which may alter content. The journal's standard [Terms & Conditions](#) and the [Ethical guidelines](#) still apply. In no event shall the Royal Society of Chemistry be held responsible for any errors or omissions in this *Accepted Manuscript* or any consequences arising from the use of any information it contains.

1 Codelivery of doxorubicin and p53 by biodegradable micellar
2 carriers based on chitosan derivatives

3 Guan-Hai Wang,^{a,b,1} Hui-Kang Yang,^{c,1} Yi Zhao,^d Da-Wei, Zhang^{e,*}

4 Li-Ming Zhang^{f,*} and Jian-Tao Lin^{a,b,*}

5 ^aDongguan Scientific Research Center, Guangdong Medical University, Dongguan
6 523808, China

7 ^bGuangdong Key Laboratory for Research and Development of Natural Drugs,
8 Guangdong Medical University, Zhanjiang 523024, China

9 ^cDepartment of Radiology, Guangzhou First People's Hospital, Guangzhou Medical Univ
10 ersity, Guangzhou 510180, China

11 ^dDepartment of Microbiology and Immunology, School of Basic Medicine, Guangdong
12 Medical University, Dongguan 523808, China

13 ^eDepartment of Pharmacology, School of Medicine, Guangdong Medical University,
14 Dongguan 523808, China

15 ^fDSAPM Lab, PCFM Lab, Institute of Polymer Science, School of Chemistry and
16 Chemical Engineering, Sun Yat-sen University, Guangzhou 510275, China

17
18
19 Keywords: chitosan, micellar carriers, codelivery

20
21 * To whom correspondences should be addressed: D.w.zhang@163.com (Zhang D);
22 ceszhlm@mail.sysu.edu.cn (Zhang); linjt326@163.com (Lin)

23 Other authors' email addresses: wanggh0101@163.com (Wang G.),
24 123086302@qq.com (Yang), zhaoyicomnet@gmail.com (Zhao),

25 ¹ These authors contributed equally to this work.

26

27

28

29

30 Abstract

31 In this work, novel biodegradable cationic micelles were prepared based on poly-(N-
32 ϵ -carbonyloxy-L-lysine) (PZLL) and chitosan (CS) by click reaction, and applied for
33 co-delivery doxorubicin (DOX) and p53 plasmid. The structure of copolymer was
34 characterized by ^1H NMR, FTIR. The loading amount of DOX in micelles was 12.8%.
35 Fluorescence spectra confirmed DOX interact π - π stacking with micelles when DOX was
36 encapsulated into the micelles. In particular, its complexation with plasmid DNA was
37 investigated by agarose gel electrophoresis, flow cytometry, zeta potential, and particle
38 size analyses as well as transmission electron microscopy observation. The results
39 showed that the copolymers have strong pDNA condensation ability and protection of
40 pDNA against deoxyribonuclease I degradation. CS-g-PZLL/DOX/p53 nanoparticles
41 showed good gene transfection efficiency in vitro. Fluorescence images and flow
42 cytometry test revealed p53 and DOX could be efficiently transported into HeLa tumor
43 cells simultaneously, and the optimum N/P ratio for p53 transfection was 20/1. For co-
44 delivery analysis, the obtained CS-g-PZLL/DOX/p53 complexes showed a better
45 inhibition effect on HeLa tumor cells than DOX or p53 used singly.

46

47

48

49

50

51

52

53

54

55

56 1. Introduction

57 So far, cancer treatment still faces serious challenge. Chemotherapy is one of
58 reliable choices for the treatment of many cancers. However, the treatment of
59 chemotherapy has been limited because of the emergence of multi-drug resistance(MDR),
60 which commonly associates with cancer cell overexpression of drug transporter
61 proteins.[1] A novel approach to address cancer drug resistance is to take the advantage
62 of the co-delivery of anticancer drugs and nucleic acid using multi-functionalized
63 nanocarriers. Co-delivery of the anticancer drugs and nucleic acid to the tumor site could
64 efficiently control the drug transporter proteins. This promising way may sidestep MDR
65 and lead to an improved therapeutic effect.

66 For the co-delivery of drugs and gene while maintaining their biological functions,
67 there has been an increasing interest in the development of multifunctional polymeric
68 carriers by using polymers [2-4] , liposomes [5-6] dendrimers [7-8], silica [9-10],
69 quantum dots [11]based nanoparticles and so on. As one of the most promising
70 nanocarrier systems, self-assembled cationic polymeric micelles were widely utilized as
71 drug and gene co-delivery systems. Cationic micelles are very effective nano-carriers for
72 the co-deliver of gene and drugs into various cancer cell lines. Shi et al. prepared a series
73 of cationic micelles based on triblock copolymers (MPEG-PCL-g-PEI) to deliver
74 doxorubicin and gene Msurvivin T34A. Their results showed that DOX and gene were
75 successfully co-delivered to the MCF-7 and CT26 cells. By introduction of T34A in
76 combination with doxorubicin, it could greatly reduce systemic toxicity as well as
77 improve the anti-tumor efficiency[12]. Lee et al. designed an amphiphilic copolymer
78 poly{(N-methyldietheneamine sebacate)-co-[(cholesteryl oxocarbonylamido ethyl)
79 methyl bis[13] ammonium bromide] sebacate} [P(MDS-co-CES)] to deliver human
80 TRAIL and paclitaxel simultaneously. They found the co-delivery nanoparticulate system
81 induced synergistic anti-cancer activities with relatively low toxicity in non-cancerous
82 cells[14]. However, these kind of cationic polymers are still associated with problems of
83 biodegradability, biocompatibility and cytotoxicity, which need to be overcome for in
84 vivo application.

85 In this work, novel cationic micelles based on the polysaccharide and polypeptide
86 were prepared by click chemistry, and applied for co-delivery of doxorubicin (DOX) and

87 p53 plasmid. Poly-(N- ϵ -carbobenzyloxy-L-lysine) (PZLL) is a hydrophobic derivate of
88 polypeptide. Due to their good biocompatibility and biodegradability, PZLL have been
89 widely used as the hydrophobic inner cores of micelles [15-17]. DNA can be bound
90 tightly to the surfaces of the micelles because of the amino groups in chitosan chains and
91 PZLL branch chains. Their proton buffering capability, DNA condensation ability,
92 protection of pDNA against deoxyribonuclease I degradation, in vitro cytotoxicity and
93 gene transfection efficiency into Hela cells were investigated via acid–base titration,
94 agarose gel electrophoresis, MTT, flow cytometry assay and fluorescence microscope.
95 Their drug loading capacity and in vitro release behavior were studied using DOX as a
96 model drug. The co-delivery of an anti-cancer DOX and functional gene (p53 plasmid)
97 into Hela cells was also investigated and discussed in this study.

98 2. Experimental section

99 2.1. Materials

100 N- ϵ -Carbobenzyloxy-L-lysine, doxorubicin hydrochloride, azido propylamine
101 Phthalic anhydride, hydrazine monohydrate, N-bromosuccinimide(NBS),
102 triphenylphosphine (TPP), copper sulfate, 1-methy-2-pyrrolidinone (NMP) and
103 triphosgene were purchased from Aladdin Chemical Reagent Co., Ltd. (China). Chitosan
104 (Mw = 10 kDa) was purchased from Haidebei Marine Bioengineering Co. Ltd. (China).
105 Propargylamine, Sodium azide (NaN₃, 99%) and sodium ascorbate (99%) were purchased
106 from Alfa Aesar. The Dulbecco's modified Eagle medium (DMEM), trypsin-
107 ethylenediaminetetraacetic acid (Trypsin-EDTA), and fetal bovine serum (FBS) were
108 purchased from Gibco-BRL (Canada). Polyethylenimine (PEI, 25 kDa), 3-[4,5-
109 dimethylthiazol- 2-yl]-2,5-diphenyltetrazolium bromide (MTT) were obtained from
110 Sigma-Aldrich (U.S.A.). Deoxyribonuclease I (DNaseI) was purchased from Feibo Life
111 Sciences (China). The plasmid p53 was obtained from Invitrogen. All other reagents were
112 analytical grade and were used as received.

113 2.2. Preparation of CS-g-PZLL copolymers

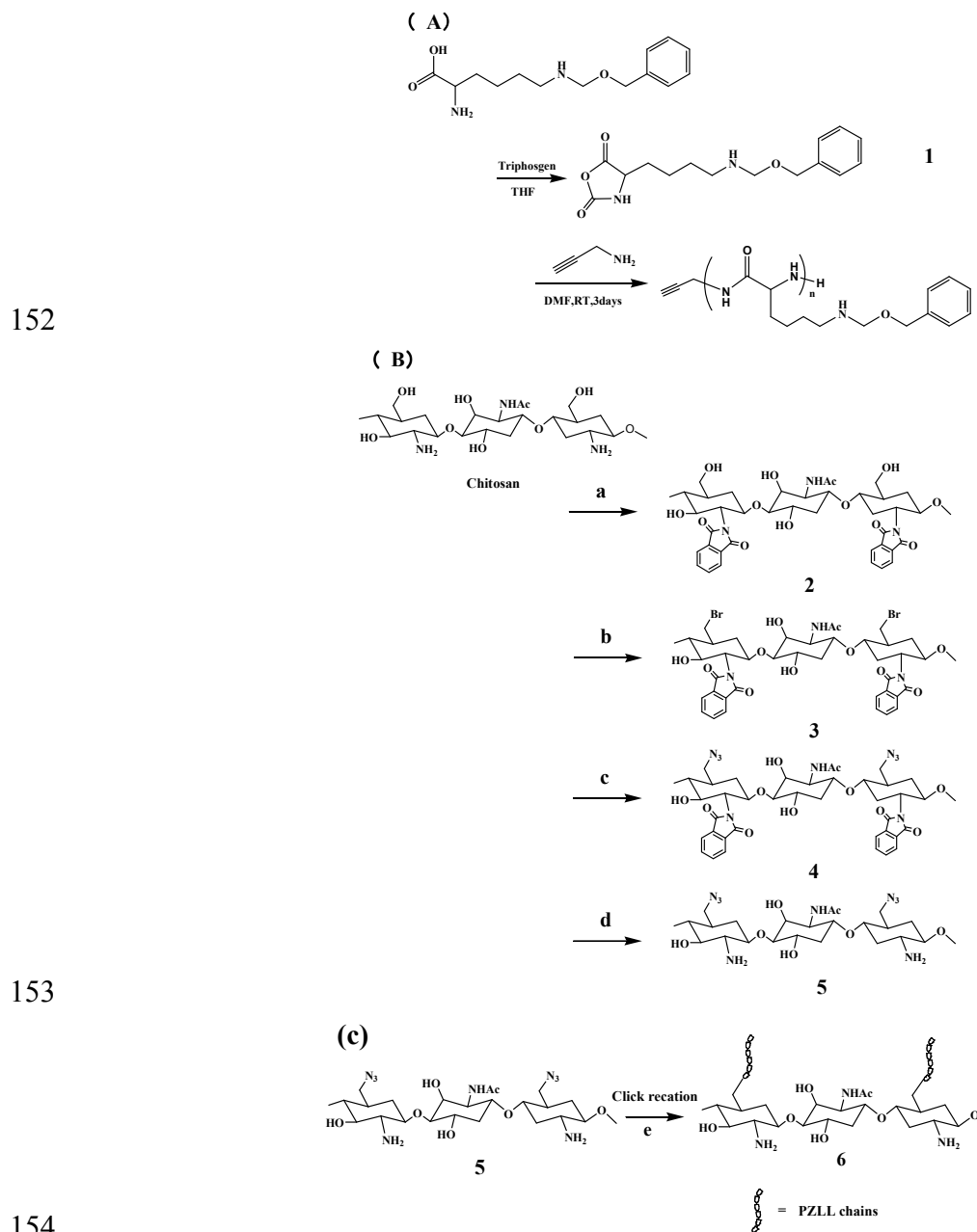
114 CS-g-PZLL were prepared by click reaction of α -alkyne-poly-(N- ϵ - carbobenzyloxy-
115 L-lysine) (α -alkyne-PZLL) and azide focal point chitosan (6-N₃-CS), as shown in Scheme
116 1. First, α -alkyne-PZLL (Scheme 1A) was synthesized following a procedure reported by
117 Lin [18].

118 In brief, 5.0 g N- ϵ -carbobenzyloxy-L-lysine (17.8 mmol) was reacted with 3g
119 triphosgene (10.1 mmol) by using tetrahydrofuran (THF) as solvent. The reaction time
120 was 1h and reaction temperature was 50 °C. After reaction, solvent was removed in
121 vacuo, the obtained residue was first dissolved in ethyl acetate, then washed with cold 5%
122 NaHCO₃ solution. The ethyl acetate layer was collected and dried by anhydrous Na₂SO₄.
123 Ethyl acetate was removed in vacuo and a ϵ -carbobenzyloxy-L-lysine N-
124 carboxyanhydride (Lys (Z)-NCA) white solid with a yield of 77% was obtained. After
125 that, 1.0 g Lys (Z)-NCA was reacted with 0.01 g propargylamine in anhydrous
126 dimethylformamide (DMF), the reaction time was 3 days. After reaction, methanol was
127 added into solution and white powder deposit was obtained. The chemical structure was
128 confirmed by ¹H NMR and FTIR. ¹HNMR (400 MHz, D₂O): δ 7.36–7.41 (5H, m -Ph),
129 5.08 (s, 2H, -OCH₂Ph), 3.95 (s, 2H, -CCH₂NH-), 2.89 (d, 2H, -NHCH₂CH₂), 1.7 (t, 2H, -
130 CHCH₂CH₂-), 1.24 (m, 2H, -CHCH₂CH₂-). IR (KBr, cm⁻¹): 3299, 3053, 2970, 1645, 1544,
131 1258, 1165, 1013, 539.

132 Second, 6-N₃-CS (Scheme 1B) was synthesized by the similar method reported by
133 Deng et al[19]. In brief, chitosan and phthalic anhydride was dissolved in DMF and
134 reacted for 8h at 120 °C to obtain N-phthaloyl-chitosan (2), (2) was then reacted with N-
135 bromosuccinimide to obtain 6-bromide-6-deoxy-N-phthaloyl-chitosan (3), after that, (3)
136 was reacted with sodium azide in N-methylpyrrolidone for 8h at 80 °C. After reaction,
137 the solution was filtered and precipitated with ethanol, precipitate was collected and
138 washed by acetone for three times, then dried under a vacuum to get 6-Azido-6-deoxy-
139 Nphthaloyl-chitosan (4) with a yield of 73%. ¹HNMR (400 MHz, D₂O): δ 3.30-3.90 (m,
140 D-glucosamine unit, H-3, H-4, H-5, H-6, H-6O), 3.34-3.78 (2H, -CONHCH₂-), 2.90
141 (protons next to amines). IR (KBr, cm⁻¹): 3442, 2930, 2114, 1667, 1382, 1071, 1013, 657.

142 At last, CS-g-PZLL was synthesized by Scheme 1C. α -alkyne-PZLL(3 mmol), 6-N₃-
143 CS (1 mmol) and the catalyst (CuSO₄·5H₂O/sodium ascorbate, 0.5 mmol/1 mmol) were
144 dissolved in 20.0 mL DMSO/water (5:1, v/v) mixture solution and reacted at 50 °C for 24
145 h. The mixture was then precipitated with ethanol and purified by dialysis in water for 2
146 days. After dialysis and lyophilization, the CS-g-PZLL was collected as a brown powder
147 with a yield of 87%. ¹HNMR (400 MHz, D₂O): δ 7.36–7.41 (5H, m -Ph), 5.08 (s, 2H, -

148 OCH_2Ph), δ 3.30-3.90 (m, D-glucosamine unit, H-3, H-4, H-5, H-6, H-60), 3.34-3.78 (2H,
 149 $-\text{CONHCH}_2-$), 2.90 (protons next to amines) 1.7 (t, 2H, $-\text{CHCH}_2\text{CH}_2-$), 1.24 (m, 2H,
 150 $\text{CHCH}_2\text{CH}_2-$). IR (KBr, cm^{-1}): 3299, 3053, 2930, 1645, 1382, 1258, 1165, 1013, 539.
 151



152

153

154

155

156

Scheme 1 Synthesis route to CS-g-PZLL

Reaction conditions: (a) phthalic anhydride, DMF, 120 °C, 8 h; (b) N-bromosuccinimide,

157 triphenylphosphine, NMP, 80 °C, 2 h; (c) sodiumazide, NMP, 80 °C, 4 h; (d) hydrazine
158 monohydrate, water, 100 °C, 10 h; (e) CuSO₄·5H₂O/sodium ascorbate, DMSO/water, 40
159 °C, 24 h.

160 2.3. DOX loading and in vitro release

161 DOX was loaded by using a dialysis method reported by Lin et al[9]. Briefly, 10mg
162 CS-g-PZLL and 5.0 mg DOX hydrochloride were first dissolved by using 5.0 mL DMSO
163 as solvent, for neutralization of HCl, a drop of triethylamine was then added to the
164 solution. The complete dissolved solution was then transferred to a dialysis bag (MWCO
165 3000) and subjected to dialysis against distilled water for 48 h. After that, the dialysis
166 solution was filtered through a 0.45 μm filter and then lyophilized. To investigate the
167 interactions between CS-g-PZLL and DOX, the obtained CS-g-PZLL/DOX complex was
168 analysed by fluorescence spectra. The excitation wavelength was 330 nm and the
169 fluorescence emission spectra were recorded in the range from 400 to 700 nm. To
170 determine the loading amount of DOX, the obtained DOX/CS-g-PZLL was dissolved in
171 DMSO and analyzed by UV–vis spectrophotometry (TU-1900, China) at 480nm. It was
172 found that the loading amount of DOX was 12.8 %. The loading amount of DOX was
173 calculated according to the following equation:

$$174 \quad LC = M_1 / M_0 \times 100\%$$

175 where M_0 is the weight of micells, M_1 is the weight of the loading DOX.

176 The release of DOX from CS-g-PZLL was assayed at 37 °C in PBS buffer of pH 5.8
177 (simulate pH of tumor) and 7.4 (simulate pH of blood plasma). Predetermined amount of
178 the DOX/CS-g-PZLL complexes in 5.0 mL of PBS (pH 5.0 and 7.4) was sealed in a
179 dialysis bag (MWCO=3KDa), then the dialysis bag was submerged in 20 mL of the
180 corresponding buffer. At predetermined time intervals, 2.0 mL of aqueous solution was
181 taken out for drug concentration measurement and replaced by an equal volume of fresh
182 PBS. The released DOX in the incubation buffer was analyzed using a UV–vis
183 spectrophotometry (TU-1900, China) at 480 nm. All measurements were performed in
184 triplicate.

185 2.4. Plasmid binding

186 2.4.1. Formation

187 For the plasmid binding to the CS-g-PZLL, p53 solution was added to the CS-g-
188 PZLL or DOX loaded CS-g-PZLL solutions at various N/P ratios, then mixed by gentle
189 agitation for 5 s and incubation at 37 °C for 30 min before used.

190 2.4.2. Gel electrophoresis

191 Agarose gel retardation assay was carried out to determine the DNA condensation
192 ability of CS-g-PZLL micellar nanoparticles to p53. CS-g-PZLL/p53 complexes were
193 prepared at various N/P ratios (CS-g-PZLL to p53: 5, 10 and 20). The complexes were
194 mixed with appropriate amounts of loading buffer and incubated for 30 min at room
195 temperature , then loaded onto 1.0 % agarose gel containing GeneGreen (0.1mg·mL⁻¹,
196 Sigma) and electrophoresed with tris-acetate buffer for 30 min at 100 V. The location of
197 DNA in the gel was analyzed using a UV transilluminator and a digital imaging system
198 (Fisher Scientific, PA, USA).

199 DNase I was added to CS-g-PZLL/p53 complexes (N/P 5, 10 and 20) for examining
200 the protection ability of CS-g-PZLL against DNase degradation. DNase I and complexes
201 were incubated at 37 °C for 30 min, after that, EDTA (4.0 mL, 250 mM) and sodium
202 dodecyl sulfate (SDS) solution (4.0 mL,10%, w/v) was added and the mixture was
203 incubated at room temperature for another 1 h. The samples were then electrophoresed on
204 the 1.0 % agarose gel to examine the integrity of DNA.

205 2.4.3. Size and morphology

206 The particle size and surface charge of the complexes were determined by a Zeta
207 Potential Analyzer instrument (ZetaPALS, Brookhaven Instruments Corporation, USA).
208 The morphology of the complex was observed by a JEM-2010HR high-resolution
209 transmission electron microscope instrument.

210 2.4.4. In vitro transfection

211 For transfection, Hela cells were plated in 24-well plates at 1×10^4 cells/well. Prior to
212 transfection, the cells were washed once with PBS buffer, and the medium in each well
213 was replaced with serum-free media for 12h. After that, Cells were replenished with 10%
214 fetal bovine serum media containing CS-g-PZLL/p53 complexes at different N/P ratios
215 (containing 2.0 µg p53 in each N/P ratio). After 48 h transfection at 37 °C, the cells were
216 observed with a Olympus IX71 fluorescence microscope (Melville, NY, U.S.A.). The
217 transfected cells were washed once with PBS, detached with 0.25% trypsin and collected,

218 transfection efficiency was analyzed via flow cytometry quantitatively by scoring the
219 percentage of cells expressing GFP (FACS Aria flow cytometer Germany).

220 2.5 In vitro Cytotoxicity Assay

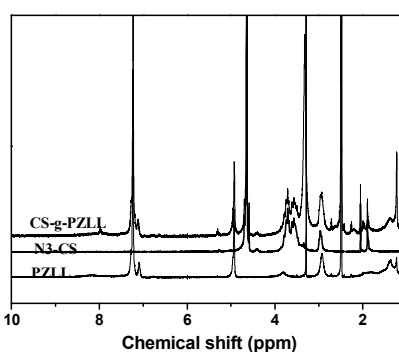
221 In vitro Cytotoxicity assay of CS-g-PZLL and DOX loaded CS-g-PZLL
222 nanoparticles was performed against Hela cells by MTT assay. Five multiple holes were
223 set for every sample. Briefly, Hela cells were respectively cultured onto 96-well plates at
224 a density of 1×10^4 cells/well and incubated in a humidified atmosphere of 5% CO₂ at 37
225 °C for 12 h. After that, the growth medium was replaced by 100 μL complete DMEM
226 containing indicated amount of sample and and further incubated for 24 h. Then 10 μL of
227 MTT ($0.5 \text{ mg} \cdot \text{mL}^{-1}$) in PBS solution was added to each well, the cells were incubated for
228 another 4h to form formazan crystals. Finally, the medium was removed and 100 μL of
229 DMSO was added to each well. The optical density values of the samples were measured
230 at 490 nm by using a MRX-Microplate Reader (Thermo, USA). The cells treated with the
231 same amount of PBS were used as control. The relative cell viability was calculated as
232 follow:

$$233 \quad \text{Cell viability (\%)} = [A_{490}(\text{sample}) / A_{490}(\text{control})] \times 100$$

234 Where $A_{490}(\text{sample})$ and $A_{490}(\text{control})$ were obtained in the presence and absence
235 of sample, respectively.

236 3. Result and discussion

237 3.1. Synthesis and characterization of CS-g-PZLL

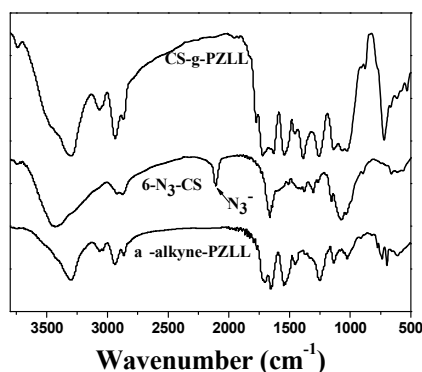


238

239 Figure 1. ¹H NMR spectra of CS-g-PZLL, N₃-CS and PZLL.

240 Figure 1 shows ¹H NMR spectra of the CS-g-PZLL, 6-N₃-CS, and PZLL. As seen in
241 the spectrum of the CS-g-PZLL, the new peaks at 5.0, 7.0-7.30 ppm showed the presence
242 of the PZLL compared to the spectrum of 6-N₃-CS. Moreover, the peak at 8.1 ppm in the

243 spectrum of the CS-g-PZLL indicated the presence of the triazole proton, which could be
244 attributed to the formation of 6-N₃-CS and PZLL by the click reaction.



245

246

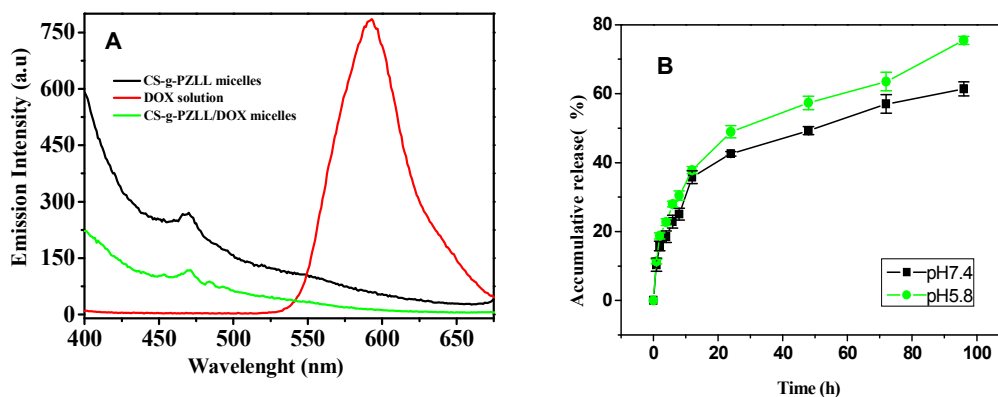
Figure 2. FTIR spectra of CS-g-PZLL, N₃-CS and PZLL.

247

248 Figure 2 shows the FTIR spectra of the CS-g-PZLL, N₃-CS and PZLL. As seen in
249 FTIR spectrum of N₃-CS, the characteristic vibration band for azide group at 2110 cm⁻¹
250 demonstrated that azide groups were successfully incorporated in N₃-CS. The new peak
251 at 1450 cm⁻¹ appeared in the samples of CS-g-PZLL, which is attributed to the 1,2,3-
252 triazole structure formed during click modification, respectively[20-21]. The FTIR data
253 indicated that the PZLL dendrimer was successfully grafted onto chitosan chains via click
254 chemistry.

254

3.2. DOX-loaded micelles and in vitro drug release

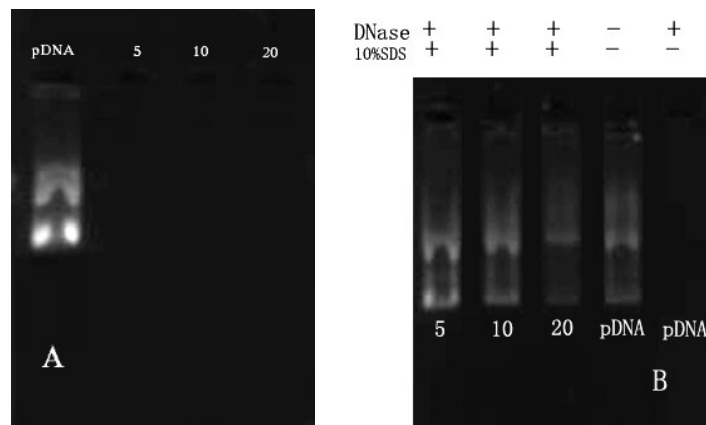


255

256 Figure 3 (A) The fluorescence spectra of the micells, DOX solution and complex
257 ($\lambda_{\text{excitation}}=330$ nm). (B) In vitro release profiles of the loading DOX from CS-g-PZLL
258 nanoparticles in phosphate buffer (pH 7.4 or 5.8) at 37 °C

259 In vitro release of drugs from micelles were investigated in pH 7.4 and 5.0 to imitate
 260 the pH of blood and tumor site. DOX was chosen as the model drug, and DOX was
 261 encapsulated into the hydrophobic core of the micelles. Figure 3(A) shows the interaction
 262 of DOX and micelles by fluorescence spectra. It was found that the fluorescence of
 263 complex was nearly completely quenched when DOX was encapsulated into the micelles,
 264 confirming the π - π stacking interaction between DOX and phenyl groups of PZLL
 265 chains[22-23]. Moreover, the π - π stacking interaction helps to improve high loading
 266 amount of DOX. It was found that the loading amount of DOX in micelles was 12.8%. As
 267 shown in Figure 3(B), release profiles showed sustained release behaviors of DOX at pH
 268 7.4 and pH 5.0. 35.7% and 37.8% of the loaded DOX were released at pH 7.4 and pH 5.0
 269 in the initial 12 h, and the accumulated release reached 61.4% and 75.4% after 96 h,
 270 respectively (Figure 3B). It is interesting to find that the release rate and released amount
 271 of DOX at pH 5.0 were a little higher than those at pH 7.4, which revealed a promoted
 272 drug release behavior at the tumor site. DOX released from micelles mainly by free
 273 diffusion. The better solubility of DOX at pH 5.0 than at pH 7.4 promoted the rapid
 274 release behavior. Moreover, the pH-responsive property of the copolymers leads to the
 275 higher release rate in lower pH. Since tumor shows lower extracellular pH, this
 276 observation demonstrated that the CS-g-PZLL micelle might show potential applications
 277 as a tumor-targeting drug delivery platform.

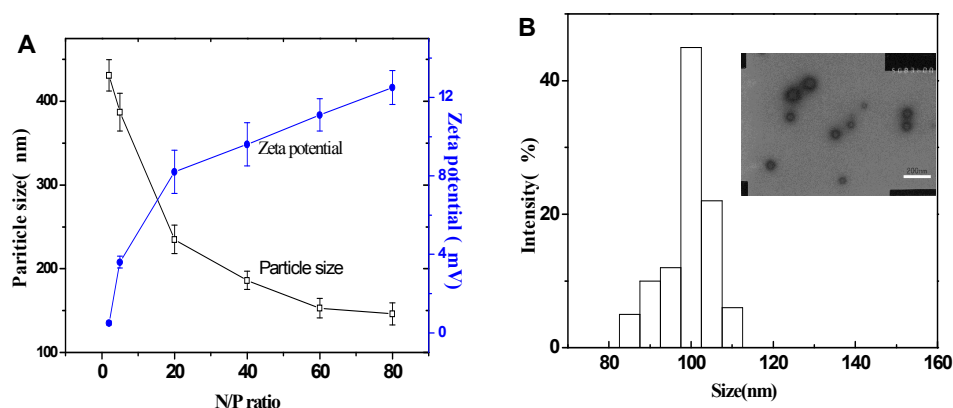
278 3.3.1 Gel electrophoresis



279 Figure 4. (A) Agarose gel electrophoresis retardation assay of CS-g-PZLL/p53
 280 complexes at different N/P ratios. (B) Protection and release assay of p53. p53 was
 281 released by adding 10% SDS to CS-g-PZLL/p53 complexes at different N/P ratios.
 282

283 The formation of CS-g-PZLL/p53 complexes was examined by agarose gel
284 electrophoresis assay. As shown in Figure 4A, the migration of pDNA was completely
285 retarded when the MSN-x-G3/pDNA weight ratio exceeded 5. These results indicated
286 that CS-g-PZLL has a strong binding ability to p53. Figure 4B shows the protection effect
287 of CS-g-PZLL against p53 degradation by DNase I. It was found that the naked p53 was
288 completely digested, while CS-g-PZLL/p53 at all N/P ratios (5, 10 and 20) exhibited
289 distinct protective effects against DNase I. These results indicated that the micells formed
290 by CS-g-PZLL copolymer could be used as a co-delivery system for loading hydrophobic
291 drugs and gene. Moreover, the co-delivery system could protect genes against DNase
292 simultaneously.

293 3.3.2. Size and morphology



294
295 Figure 5. (A) Particle sizes and zeta potentials of CS-g-PZLL/DOX/p53 complexes
296 formed at various N/P ratios. (B) Typical particle size distribution and TEM image of the
297 CS-g-PZLL/DOX/p53 complex formed at an N/P ratio of 20.

298 The mean particle sizes and zeta potential of CS-g-PZLL/DOX/p53 complexes were
299 investigated by Zeta Potential Analyzer and TEM, as shown in Figure 5. It was found that
300 the zeta potential increased with the N/P ratio of 2-80, and the range was between 0.5-
301 12.5 mV. By contrast, the size of the complexes tended to decrease with the increase of
302 N/P ratio, and remained in the size range from 400 to 150 nm. The TEM photos showed
303 that CS-g-PZLL/DOX/p53 complexes (Figure 5 B) have a spherical shape and compact
304 structure. The complexes had an average diameter of about 100 nm, which was consistent
305 with the results measured by zeta potential test. It is reported that the size range of pDNA
306 containing complexes from 50 to 400 nm was suitable for cellular endocytosis[24]. In this

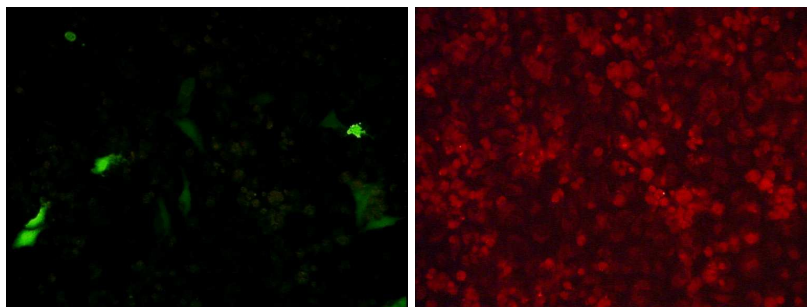
307 study, the test result of CS-g-PZLL/DOX/p53 could meet the requirement of efficient
308 gene delivery.

309 3.3.3 Co-delivery and cell viability

310

A

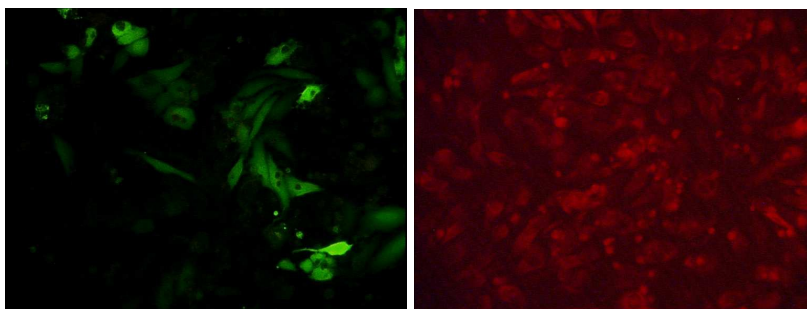
1



311

312

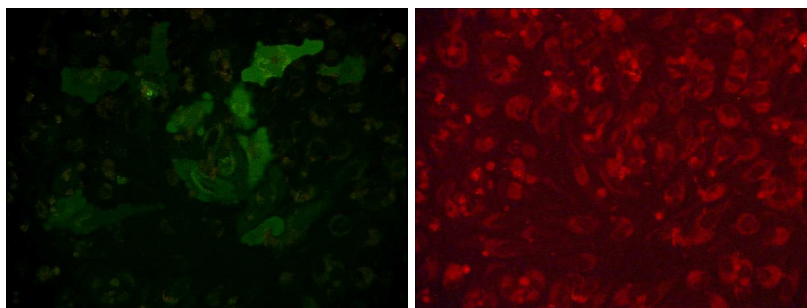
2



313

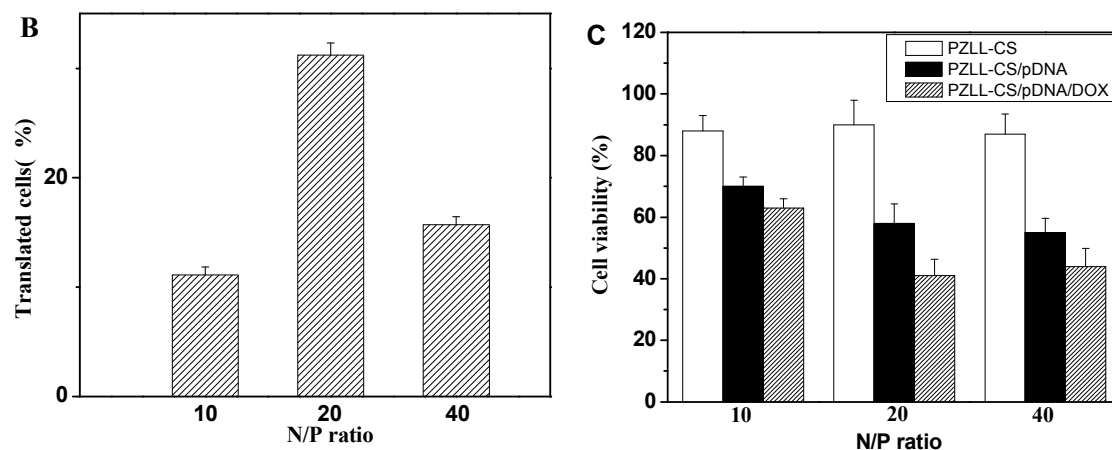
314

3



315

316



317

318 Figure 6. (A) Fluorescence field images of HeLa cells transfected by CS-g-
 319 PZLL/p53/DOX complexes formed at various N/P ratios (1 N/P=10, 2 N/P=20, 3 N/P=40).

320 (B) Quantitative determination of transfected HeLa cells by flow cytometry (C) HeLa cells
 321 viability treated by CS-g-PZLL, CS-g-PZLL/p53 and CS-g-PZLL/p53/DOX

322 To investigate the co-delivery ability of CS-g-PZLL, HeLa cells were studied by
 323 fluorescence microscopy using plasmid eGFP-N1-53 and DOX as model gene and
 324 hydrophobic drug. The representative fluorescence images are shown in Figure 6. The
 325 green and red fluorescence were both observed in the HeLa cells at different N/P ratios, the
 326 green fluorescence was from eGFP and the red fluorescence was from DOX (Figure 6 A).
 327 The results suggested that both p53 and DOX can be delivered into HeLa cells by CS-g-
 328 PZLL at different N/P ratios. The intensity of the red fluorescence at different N/P ratios
 329 did not show apparent difference. It is suggested that DOX could be efficiently
 330 transported into cells by at all N/P ratios. On the other hand, the intensity of the green
 331 fluorescence from eGFP was stronger at N/P ratio of 20 than others, indicating that N/P
 332 ratio of 20 was the optimum N/P ratio for p53 transfection. This result was consistent
 333 with the results of flow cytometry, as shown in figure 5 B. The highest transfected ratio
 334 was 31.2% while the N/P ratio was 20. The transfected cells at the N/P ratio of 40 were
 335 slightly less than those at the N/P ratio of 20. This result may be caused by the slightly
 336 reduced tolerance of HeLa cells under the high CS-g-PZLL concentration (figure 6 C).

337 The co-delivery of drug and gene has become the primary strategy in cancer and
 338 other disease therapy in recent years, because this technique could promote synergistic
 339 actions, improve target selectivity and deter the development of drug resistance. For the

340 co-delivery of antitumor drugs and genes while maintaining their chemophysical
341 properties and biological functions, a multifunctional carrier which could load gene and
342 drug simultaneously is necessary. In previous studies, cationic polymeric micelles have
343 been widely used as drug and gene co-delivery carriers. Zhu et al.[26] prepared
344 biodegradable cationic micelles based on the self-assembly of PDMAEMA-PCL-
345 PDMAEMA triblock copolymers as siRNA and paclitaxel co-delivery carriers. The
346 results demonstrated that combinatorial delivery of VEGF siRNA and paclitaxel showed
347 an efficient knockdown of VEGF expression. Zheng et al.[27] prepared polypeptide
348 cationic micelles based on poly(ethylene glycol)-*b*-poly(L-lysine)-*b*-poly(L-leucine)
349 (PEG-PLL-PLLeu) triblock copolymers as docetaxel (DTX) and siRNA-Bcl-2 co-
350 delivery vectors. The results showed that the co-delivery of DTX and siRNA-Bcl-2
351 (siRNA that suppresses the expression of anti-apoptotic Bcl-2 gene) significantly
352 inhibited tumor growth as compared to the individual siRNA or DTX treatment.

353 To confirm the cell inhibition effect of complexes containing both DOX and p53, we
354 evaluated their cytotoxic effects using a MTT assay. The results showed that CS-g-PZLL
355 was non-toxicity at the concentration of this assay, while the samples containing p53
356 showed an obvious cytotoxicity, the cell viability was decrease to 70, 58 and 55% at N/P
357 ratio of 10, 20 and 40 (Figure 6C). The further inhibition effect was found by the co-
358 delivery group, the cell viability was decrease to 63, 41 and 44% respectively. The better
359 effect may attribute to that the released DOX could damage DNA; meanwhile, p53 could
360 instigate mRNA to down-regulate protein expression. The result suggested that the co-
361 delivery induce synergistic actions and lead to an effective method for tumor therapy.

362 4. Conclusion

363 For the co-delivery of anti-tumor drug and gene to tumor cells, a new cationic
364 micelle consisting of poly-(N- ϵ -carbobenzyloxy-L-lysine) (PZLL) and chitosan has been
365 synthesized, and used to co-deliver DOX and p53 for cancer therapy. CS-g-
366 PZLL/DOX/p53 nanoparticles showed good gene transfection efficiency in vitro, and
367 could delivered p53 and DOX simultaneously to Hela tumor cells. For co-delivery
368 analysis, the obtained CS-g-PZLL/DOX/p53 complexes showed a better
369 inhibition effect on Hela tumor cells than p53 used singly. Such a cationic micelle deliver

370 system may be used as a potential multifunction vector for future cancer therapy
371 applications.

372 Acknowledgment

373 This work was financially supported by National Natural Science Foundation of China
374 (81402563), Traditional Chinese Medicine Bureau Foundation of Guangdong Province
375 (20141158), Doctoral Research Program of Guangdong Medical College
376 (XB1303 and XB1387) and Special Foundation for Young Innovation Scientists of
377 Department of Education of Guangdong Province(4CX14119G and 4CX14118g).

378 References

- 379 1. X.-B. Xiong and A. Lavasanifar, *ACS nano*, 2011, **5**, 5202-5213.
- 380 2. Y. Wang, S. Gao, W.-H. Ye, H. S. Yoon and Y.-Y. Yang, *Nature materials*, 2006,
381 **5**, 791-796.
- 382 3. Q.-D. Hu, H. Fan, Y. Ping, W.-Q. Liang, G.-P. Tang and J. Li, *Chemical*
383 *Communications*, 2011, **47**, 5572-5574.
- 384 4. M. Ma, Z. Yuan, X. Chen, F. Li and R. Zhuo, *Acta biomaterialia*, 2012, **8**, 599-
385 607.
- 386 5. M. S. Suh, G. Shim, H. Y. Lee, S.-E. Han, Y.-H. Yu, Y. Choi, K. Kim, I. C.
387 Kwon, K. Y. Weon and Y. B. Kim, *Journal of Controlled Release*, 2009, **140**,
388 268-276.
- 389 6. Z. Xu, Z. Zhang, Y. Chen, L. Chen, L. Lin and Y. Li, *Biomaterials*, 2010, **31**,
390 916-922.
- 391 7. S. Liu, Y. Guo, R. Huang, J. Li, S. Huang, Y. Kuang, L. Han and C. Jiang,
392 *Biomaterials*, 2012, **33**, 4907-4916.
- 393 8. T. L. Kaneshiro and Z.-R. Lu, *Biomaterials*, 2009, **30**, 5660-5666.
- 394 9. J.-T. Lin, C. Wang, Y. Zhao and G.-H. Wang, *Materials Research Express*, 2014,
395 **1**, 035403.
- 396 10. M. Akin, R. Bongartz, J. G. Walter, D. O. Demirkol, F. Stahl, S. Timur and T.
397 Scheper, *Journal of Materials Chemistry*, 2012, **22**, 11529-11536.
- 398 11. J.-M. Li, Y.-Y. Wang, M.-X. Zhao, C.-P. Tan, Y.-Q. Li, X.-Y. Le, L.-N. Ji and Z.-
399 W. Mao, *Biomaterials*, 2012, **33**, 2780-2790.
- 400 12. S. Shi, K. Shi, L. Tan, Y. Qu, G. Shen, B. Chu, S. Zhang, X. Su, X. Li and Y.
401 Wei, *Biomaterials*, 2014, **35**, 4536-4547.
- 402 13. D. G. Anderson, W. Peng, A. Akinc, N. Hossain, A. Kohn, R. Padera, R. Langer
403 and J. A. Sawicki, *Proceedings of the National Academy of Sciences of the United*
404 *States of America*, 2004, **101**, 16028-16033.
- 405 14. A. L. Lee, Y. Wang, S. Pervaiz, W. Fan and Y. Y. Yang, *Macromolecular*
406 *bioscience*, 2011, **11**, 296-307.
- 407 15. H.-Y. Wen, H.-Q. Dong, W.-j. Xie, Y.-Y. Li, K. Wang, G. M. Pauletto and D.-L.
408 Shi, *Chemical Communications*, 2011, **47**, 3550-3552.

- 409 16. J. Ding, J. Chen, D. Li, C. Xiao, J. Zhang, C. He, X. Zhuang and X. Chen,
410 *Journal of Materials Chemistry B*, 2013, **1**, 69-81.
- 411 17. C. Deng, X. Chen, H. Yu, J. Sun, T. Lu and X. Jing, *Polymer*, 2007, **48**, 139-149.
- 412 18. J.-T. Lin, Y. Zou, C. Wang, Y.-C. Zhong, Y. Zhao, H.-E. Zhu, G.-H. Wang, L.-M.
413 Zhang and X.-B. Zheng, *Materials Science and Engineering: C*, 2014, **44**, 430-
414 439.
- 415 19. J. Deng, Y. Zhou, B. Xu, K. Mai, Y. Deng and L.-M. Zhang, *Biomacromolecules*,
416 2011, **12**, 642-649.
- 417 20. J. T. Lin, Y. Zou, C. Wang, Y. C. Zhong, Y. Zhao, H. E. Zhu, G. H. Wang, L. M.
418 Zhang and X. B. Zheng, *Materials Science & Engineering C Materials for*
419 *Biological Applications*, 2014, **44**, 430–439.
- 420 21. J. Deng, Y. Zhou, X. Bo, K. Mai, Y. Deng and L. M. Zhang, *Biomacromolecules*,
421 2011, **12**, 642-649.
- 422 22. M. Dong, L. Zong-Hua, Z. Qian-Qian, Z. Xiao-Yan, Z. Yi, S. Yun-Feng, L. Jian-
423 Tao and X. Wei, *Macromolecular Rapid Communications*, 2013, **34**, 548–552.
- 424 23. D. Ma, J. Lin, Y. Chen, W. Xue and L. M. Zhang, *Carbon*, 2012, **50**, 3001–3007.
- 425 24. M. Metzke, N. O'Connor, S. Maiti, E. Nelson and Z. Guan, *Angewandte Chemie*
426 *International Edition*, 2005, **44**, 6529-6533.
- 427 25. C. Zhu, S. Jung, S. Luo, F. Meng, X. Zhu, T. G. Park and Z. Zhong, *Biomaterials*,
428 2010, **31**, 2408-2416.
- 429 26. C. Zheng, M. Zheng, P. Gong, J. Deng, H. Yi, P. Zhang, Y. Zhang, P. Liu, Y. Ma
430 and L. Cai, *Biomaterials*, 2013, **34**, 3431-3438.
- 431
- 432